

Sensitivities and Singular Vectors with Moist Norms

T. Jung¹, J. Barkmeijer¹, M.M. Coutinho², and C. Mazeran³

¹ *ECWMF, Shinfield Park, Reading
RG2 9AX, United Kingdom
thomas.jung@ecmwf.int*

² *Department of Meteorology,
Reading University, Reading,
United Kingdom*

³ *MATMECA, Bordeaux, France*

ABSTRACT

The sensitivity of forecast errors with respect to perturbations of the humidity analysis is described making use of the adjoint technique. Using different norms and adiabatic as well as diabatic versions of the tangent forward propagator (TFP) and its adjoint, it is shown that the influence on the forecast error of humidity perturbations obtained with the adjoint technique is relatively small compared to temperature, vorticity, and divergence perturbations. Moreover, the linearity of the growth of small humidity perturbations that are constrained by the background error covariance matrix is described. It is shown that already after 48 hours the growth of these humidity perturbations is significantly influenced by nonlinearities.

Further, the influence of diabatic processes and humidity perturbations on the growth of extratropical singular vectors (SVs) is described in a case study of the storm ‘Lothar’ which hit Middle Europe during Christmas 1999. In line with the results from the sensitivity analysis, the inclusion of humidity perturbations has little impact on the SVs. It has been found, however, that the growth of extratropical SVs is enhanced if diabatic processes are accounted for in the tangent linear computations.

1 Introduction

In the first part of this study sensitivity analysis based on the adjoint technique is used to determine those perturbations in the initial conditions which reduce short-range forecast errors. The basic idea is that, for a perfect model, short-range forecast errors are solely due to growing analysis errors. By integrating these forecast errors backwards in time using the forecast error as an input for the adjoint model, the growing parts of the analysis error can be determined (Rabier et al., 1996). After a few iterations this procedure yields so-called *key-analysis errors* (Klinker et al., 1998). Throughout the manuscript we use the expression *key-analysis errors*. It is stressed, though, that *key-analysis errors* represent growing parts of the analysis error only if the underlying assumptions are fulfilled (see further below).

Key-analysis errors for temperature, vorticity, divergence, and the logarithm of surface pressure (*dry variables*, hereafter) based on adiabatic evaluations of the TFP and its adjoint are operationally being determined at ECMWF since 1 April 1995. Given the increasing interest in humidity analyses along with their errors and given that errors in the humidity analysis may also have a noticeable impact on the forecast errors, primarily through diabatic processes (e.g., large-scale precipitation), it has been decided to extend the operational dry and adiabatic sensitivity suite in two respects. First, the adiabatic TFP and its adjoint are replaced by diabatic versions. Second, the norm at initial time is changed so that humidity *key-analysis errors* can be determined. In this study, we present preliminary results from research experiments based on this new moist sensitivity suite.

An important component of the Integrated Forecast System at ECMWF is the Ensemble Prediction System (EPS) (Molteni et al., 1996; Palmer, 2000). The EPS has been developed to account for the flow-dependent nature of predictability. The EPS at ECMWF is based on the so-called singular vector method, which gives a set of initial perturbation vectors that show the largest linear growth over a specified forecast range (e.g., 48 hours) and for particular norms. These SVs are used to produce 50 perturbed initial conditions from which 50 nonlinear perturbed integrations over 240 hours are being produced. These ensemble forecasts allow to quantify the predictability of the flow. For the extratropics the operational EPS does neither account for moist processes—an adiabatic TFP is used—nor are humidity perturbations part of the SVs at initial time—dry SVs are used. Motivated by the importance of moisture and diabatic processes (e.g., latent heat release through condensation), particularly in developing low pressure systems (e.g. Wernli and Davis, 1997; Wernli et al., 2002), numerical experiments with moist SVs for severe weather events have been carried out. In the second part of this study we briefly report some preliminary results from moist singular vector experiments for the storm ‘Lothar’, which had devastating effects in parts of France, Germany, and Switzerland during Christmas 1999.

2 Methods

2.1 Sensitivity

To understand the source of forecast errors, it is of some interest (among others) to know how sensitive forecast errors are with respect to small perturbations of the initial conditions. The forecast error can be quantified by means of the diagnostic function (or cost function) $J = 1/2 \langle \mathbf{x}_t - \mathbf{x}_t^{ref}, \mathbf{x}_t - \mathbf{x}_t^{ref} \rangle$, where \mathbf{x}_t denotes the forecast and \mathbf{x}_t^{ref} the verifying analysis (t=48 hours). Here we are interested in changes of J with respect to changes in the initial conditions, that is, we are interested in the gradient ∇J_0 . As shown by Rabier et al. (1996), ∇J_0 can be obtained as follows:

$$\nabla J_0 = C_0^{-1} R^* P^* C_1 P (\mathbf{x}_t - \mathbf{x}_t^{ref}), \quad (1)$$

where C_0 and C_1 are norms at initial and final time, respectively; R^* denotes the adjoint of the TFP; P (P^*) is (the adjoint of) the projection operator which is used to confine the diagnostic function to specific areas (e.g., Northern Hemisphere); and $\mathbf{x}_t - \mathbf{x}_t^{ref}$ is the forecast error at final time t . It becomes evident from Eq. (1) that the gradient depends on the following items:

- the norms used at initial and final time,
- the adjoint of the TFP and the validity of the tangent linear hypothesis,
- the area for which the forecast error is being studied,
- the difference between the forecast and the verifying analysis (forecast error).

In this study two different kind of norms are being used to constrain the structures and magnitudes of the key-analysis errors, that is, the TE norm and a norm that is based on the background error covariance matrix (B norm). The TE norm is defined as follows:

$$\langle \vec{x}, C_{TE} \vec{x} \rangle = \frac{1}{2} \int \int \left[u'^2 + v'^2 + \frac{c_p}{T_r} T'^2 + c_q \frac{L^2}{c_p T_r} q'^2 \right] d\Sigma \frac{\partial p_r}{\partial \eta} d\eta + \frac{1}{2} \int \left[R \frac{T_r}{p_r} \ln p_s'^2 \right] d\Sigma, \quad (2)$$

where u' , v' , T' , p'_s , and q' are perturbations of zonal wind, meridional wind, temperature, surface pressure and humidity, respectively (e.g., Ehrendorfer et al., 1999, for details). In this context c_q is a tuning parameter that can be used to adjust the magnitude of humidity key-analysis errors. For $c_q = 0$ we obtain the dry TE norm. For very small (large) values of c_q the magnitude of the humidity key-analysis errors becomes large (small) and key-analysis errors in the dry variables become relatively small (large). Here, $c_q = 0$ (dry TE norm) and $c_q = 0.001$ (moist TE norm) are used. Note, that the choice of $c_q = 0.001$ is somewhat arbitrary. We have

checked different values of c_q for the moist TE norm and found that a value of $c_q = 0.001$ leads to lowest values of the cost function, and the magnitude of the resulting key-analysis errors appears to be more or less well balanced for the dry variables and humidity.

The B norm, which is also used in this study, provides statistically and physically consistent increments at the neighbouring grid points and levels of the model and for different parameters. Here we use the formulation by Derber and Bouttier (1999), which is operationally used in the ECMWF 3dVar and 4dVar assimilation schemes. In the context of the present study the usage of the moist B norm instead of the moist TE norm has the advantage that no parameter (like c_q for the TE norm) has to be adjusted.

The gradient ∇J_0 can also be used to change the initial conditions in such a way that the forecast started from the perturbed analysis is better than the forecast started from the original analysis (Rabier et al., 1996). This technique can easily be extended by iteratively minimizing the cost function. This technique, which yields so-called key-analysis errors (Klinker et al., 1998), is schematically shown in Fig. 1. The forecast error measured in terms of the cost function is minimized by iteratively correcting the analysis along the direction of the steepest descent. Since analyses which are “corrected” by this technique lead to nonlinear forecasts that are better than those started from the original analysis, it can be expected—if all the assumptions are valid—that the corrected analysis is closer to the true state of the atmosphere than the original analysis.

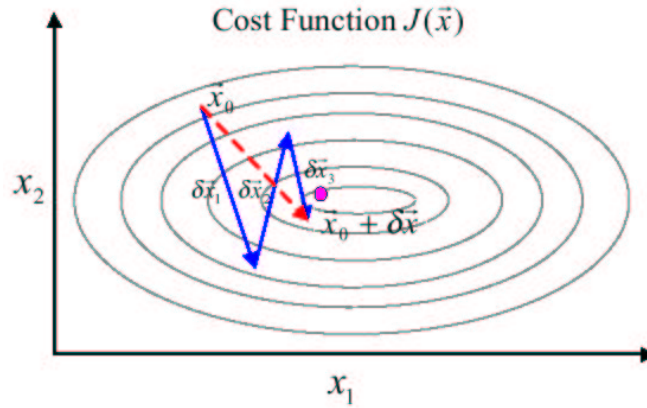


Figure 1: Concept of key-analysis error. The forecast started from the analysis leads to a relatively large forecast error. After a few updates of the analysis (blue arrows) along the direction of the steepest descent, a new “corrected” analysis has been found that leads to lower forecast errors than the original forecast. The adjoint model is essential in determining the gradients.

For the sensitivity computations we use different models, that is, an adiabatic and diabatic version of the TFP, along with their their adjoints, as well as the full nonlinear ECMWF model. The latter model is used for control and sensitivity integrations. All models are spectral (T63) with 60 levels in the vertical. The period under investigation starts at 29 April 2001 and ends at 6 June 2001. The diagnostic cost function (C_1) is based on the dry TE norm. The projection operator is used to focus the cost function on the Northern Hemisphere only. The optimization time is 48 hours.

2.2 Singular vectors

Singular vectors \mathbf{v}_0 define an unstable subspace in the tangent linear space at initial time. For given norms they represent the directions in phase space of the system that are characterized by the largest linear growth over some specified time period (optimization time). The maximizations of the perturbations growth leads to the following eigenvalue problem:

$$C_0^{-1/2} R^* C_1 R C_0^{-1/2} \mathbf{v}_0 = \sigma^2 \mathbf{v}_0. \quad (3)$$

This is equivalent to determining the SVs of $C_1^{1/2}RC_0^{-1/2}$ (therefore the name *singular vectors*). A more detailed description is given elsewhere (e.g. Buizza and Palmer, 1995; Palmer, 2000). As for the key-analysis errors, the SVs depend on the norms at initial and final time, the tangent linear model, and on the projection operator.

Here, SVs for the storm ‘Lothar’ are computed using adiabatic and diabatic linear models. The impact of initial moisture perturbations on the SVs is investigated by comparing SVs for dry and moist TE norms. As in Buizza et al. (1996) and Ehrendorfer et al. (1999) the moist TE norm is computed with $c_q = 1$ to get significant contributions from dry and moist components, both at initial and final time.

The basic state used is for 25 December 1999 at 12 UTC, and the optimization time interval is 24 hours. A projection operator (Buizza, 1994) is used to confine SVs to have maximum amplitude in the region north of 30°N. The model has a horizontal resolution of T63 and 31 levels are used in the vertical. Throughout the manuscript only the 10 leading SVs showing the largest growth will be considered.

3 Results

3.1 Sensitivity

3.1.1 Adiabatic versus diabatic key-analysis errors

As mentioned in the Introduction key-analysis errors for the dry variables are operationally being determined at ECMWF using an adiabatic version of the TFP and its adjoint. It seems likely, however, that analysis errors influence subsequent forecasts also through moist physical processes (e.g., condensation). Therefore, first the influence of physical processes in tangent linear and adjoint computations on temperature, vorticity, and divergence key-analysis errors are studied. To this end, the results from an *adiabatic* and *diabatic* sensitivity experiment using the dry TE norm at initial time are being described. The experiments cover 39 days in early summer 2001. The average reduction (averaged over all 39 cases) of the cost function (dry TE norm at final time) during the minimization for adiabatic and diabatic sensitivity is shown in Fig. 2. Using the diabatic TFP and its adjoint it clearly takes more iterations to reduce the cost function to values similar to those obtained by the adiabatic sensitivity. Throughout the remainder of this study the results based on 3 (6) iterations for (diabatic) sensitivity computations will be discussed.

The spatial structure of the key-analysis errors for temperature, vorticity and (to a lesser extent) divergence is similar for adiabatic and diabatic key-analysis errors. The average (39 cases) spatial correlation coefficient for Northern Hemisphere, mid-troposphere, adiabatic and diabatic key-analysis errors for temperature, vorticity, and divergence amounts to $r = 0.88$, $r = 0.91$, and $r = 0.69$, respectively. The magnitude of adiabatic and diabatic key-analysis errors is also very similar, as is the forecasts skill of the nonlinear sensitivity forecasts started from “adiabatically corrected” and “diabatically corrected” analyses. Thus, the characteristics of temperature, vorticity and divergence key-analysis errors seem not to be strongly affected if diabatic processes are accounted for in sensitivity computations. It should be mentioned, however, that the characteristics of humidity key-analysis errors strongly depend on the physical processes used in the adjoint calculation. In contrast to diabatic humidity key-analysis errors, adiabatic humidity key-analysis errors mirror those for temperature. It is for this similarity that all subsequent humidity key-analysis calculations are based on diabatic models.

3.1.2 Total energy norm versus B norm

In this section the influence of the choice of the norm at initial time on humidity key-analysis errors is described. The dependence of the cost function on the number of iterations for the dry TE norm and the dry B norm are shown in Fig. 2. Clearly, the reduction of the average cost function, and therefore the forecast error reduction, is very much alike for both norms.

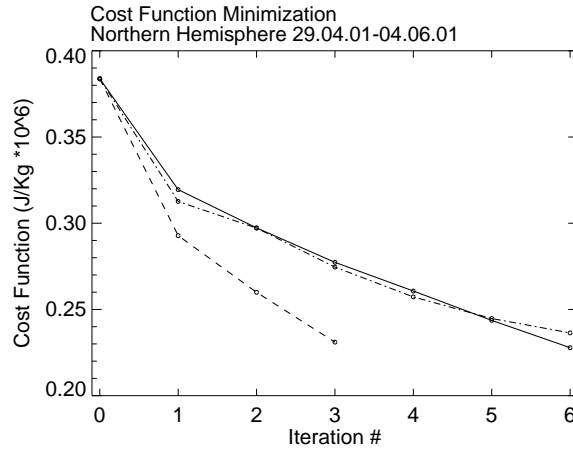


Figure 2: Cost function for diabatic sensitivity with dry TE norm (solid) and dry B norm (dash-dotted) and for adiabatic sensitivity with dry TE norm (dashed). The cost function is based on the dry TE norm and quantifies the 48 hours forecast error.

Next, the influence of the moist norm on the characteristics of humidity key-analysis errors is studied. The results are based on two diabatic sensitivity experiments, one using the moist TE norm (with $c_q = 0.001$, see Eq. 2) and the other using the moist B norm. Humidity key-analysis errors for 1 May 2001 using the TE norm (left) and the B norm (right) are depicted in Fig. 3. The norm at initial time clearly has an impact on the structure of the humidity key-analysis errors, that is, humidity key-analysis errors which are based on the TE norm are of smaller spatial scale than those based on the B norm. In line with these scale differences, regions of discrepancy between humidity key-analysis errors can be found (e.g., the Baltic Sea region). Generally, though, areas with large magnitudes of humidity key-analysis occur at similar places independent of which of the two norms is being used (e.g., central North America and central North Pacific). We note in passing that the largest differences between key-analysis errors based on the TE norm and the B norm are found for temperature; temperature key-analysis errors based on the B norm are much more large-scale than those obtained with the TE norm (not shown).

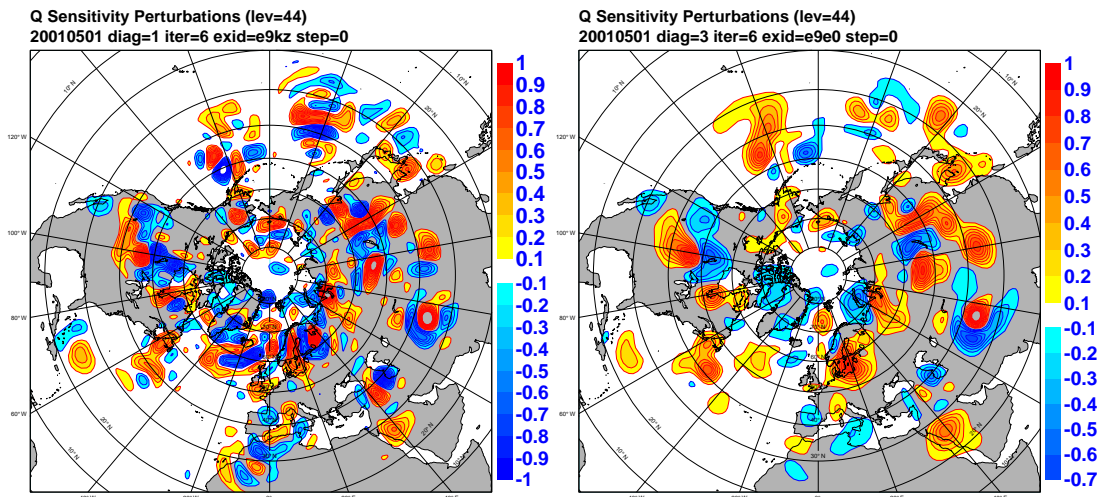


Figure 3: Humidity key-analysis errors for 1 May 2001 at about 700 hPa: Diabatic sensitivity with (left) moist TE norm and (right) moist B norm.

The standard deviation (std) of humidity key-analysis errors at about 700 hPa for the period from 29 April to 6 June 2001 using the moist TE norm (left) and the moist B norm (right) is shown in Fig. 4. Obviously, the spatial

patterns of the std of humidity key-analysis errors are very similar for both norms. Humidity key-analysis errors appear to be more or less uniformly distributed over the Northern Hemisphere. There is some zonal asymmetry, through, that is, humidity key-analysis errors are lower over eastern parts compared to western parts of the North Atlantic and North Pacific basins. Differences in the magnitude of the humidity key-analysis errors are difficult to interpret. This is because of the subjectivity that comes along with the choice of the weight (c_q in Eq. 2) that is given to humidity perturbations in the moist TE norm.

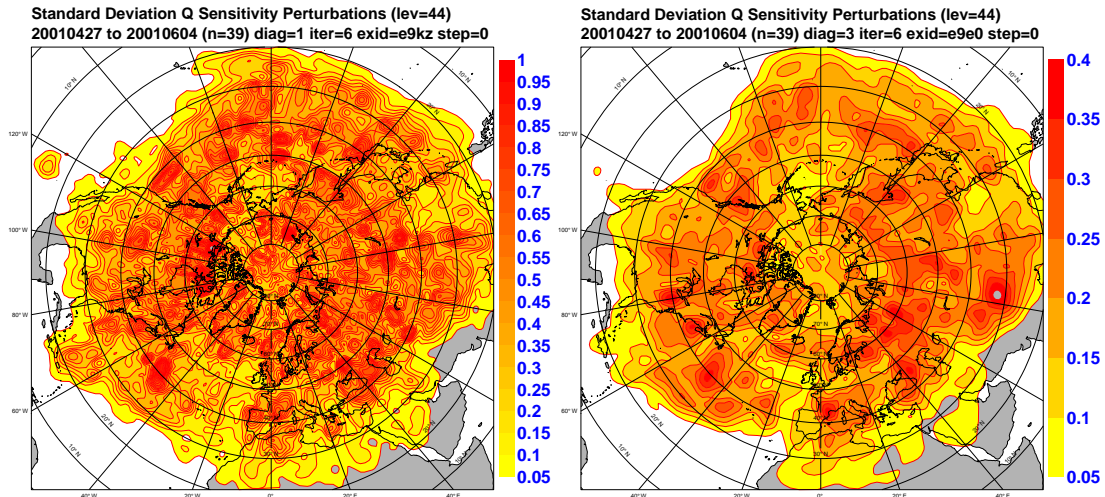


Figure 4: Standard deviation of humidity key-analysis errors (g/kg) at about 700 hPa based on the period 29 April to 6 June 2001: Diabatic sensitivity with (left) moist TE and (right) moist B norm. Note differences in colour scales.

Skill scores for the nonlinear sensitivity forecasts of Northern Hemisphere 500 hPa geopotential height fields (Z500) are shown in Fig. 5 along with those for the (unperturbed) control forecast. At this stage the focus is on dry norms to bypass the subjective that comes along with the choice of c_q and, thus, to isolate the role of the norm. Both nonlinear sensitivity forecasts have much reduced RMSE compared to the control forecast. Notice, that this implies no (average) gain in predictive skill, because one has to wait for two days to determined the forecast error, which is used to correct the analysis. Further, the nonlinear sensitivity forecast which is based on the B norm is slightly better than those based on the TE norm, suggesting that the corrected analyses using the B norm are closer to the true state of the atmosphere than those obtained by the TE-based sensitivity.

3.1.3 Dry versus moist norms

In this section we describe differences between the usage of dry (no humidity key-analysis errors) and moist (with humidity key-analysis errors) sensitivity. To this end, we have performed *diabatic* sensitivity experiments using dry and moist B norm as initial norm for the period from 29 April 2001 to 6 June 2001. The RMSE for Northern Hemisphere Z500 fields is shown in Fig. 6 for the control forecast (red), dry sensitivity (blue), and moist sensitivity (green). The additional correction of the operational humidity analysis using humidity key-analysis errors does not improve the nonlinear sensitivity forecast.

These rather neutral results on the skill scores might be interpreted in the way that diabatic adjoint sensitivity can not be used to determine meaningful (in the sense of forecast error reduction) humidity key-analysis errors. To address this item, we have performed an additional sensitivity experiment in which the B norm was changed so that only humidity key-analysis errors were determined. The skill score for nonlinear sensitivity forecasts from analyses that were corrected using humidity key-analysis errors only shows that humidity key-analysis errors are capable of reducing the forecast errors (Fig. 6, brown), although less so than dry key-analysis errors.

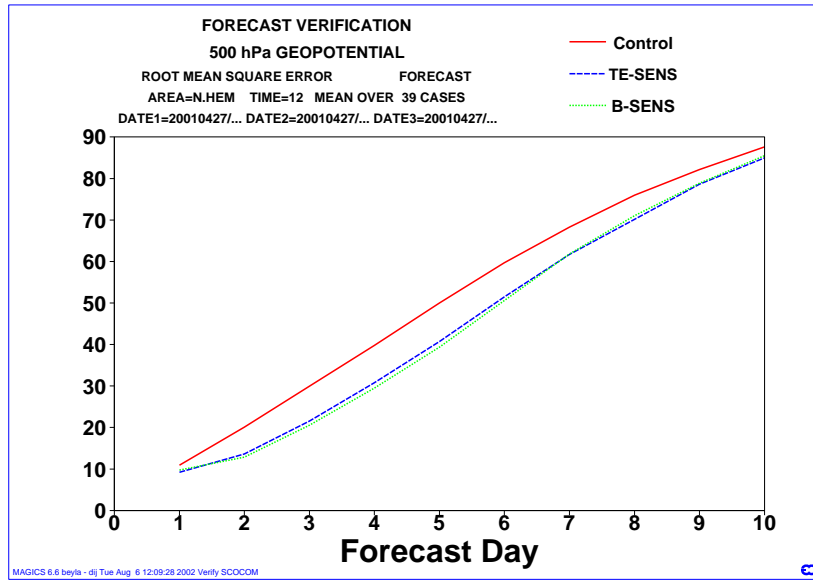


Figure 5: RMSE of Northern Hemisphere 500 hPa geopotential height fields versus forecast days: control forecast (red), nonlinear sensitivity forecast with dry TE norm (blue), and nonlinear sensitivity forecast with dry B norm. RMSE statistics are based on the period 29 April 2001 to 6 June 2001 (39 cases).

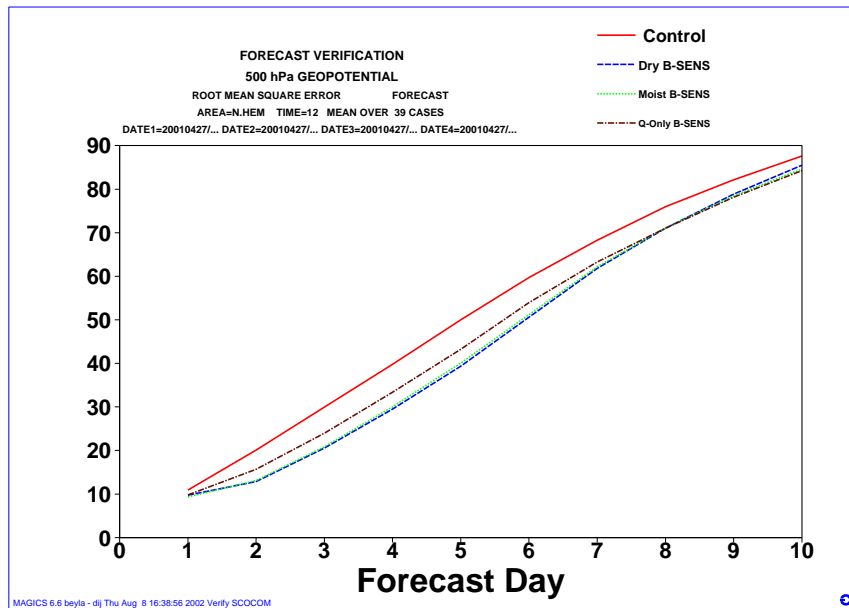


Figure 6: RMSE of Northern Hemisphere 500 hPa geopotential height fields versus forecast days: control forecast (red), nonlinear sensitivity forecast with dry B norm (blue), nonlinear sensitivity forecast with moist B norm (green), and nonlinear sensitivity forecast with humidity only B norm (brown). RMSE statistics are based on the period 29 April 2001 to 6 June 2001 (39 cases).

3.1.4 The growth of humidity perturbations

It is interesting to investigate how humidity key-analysis error influence the forecast compared to key-analysis errors of the “dry” parameters (temperature, vorticity, divergence, and surface pressure). The (spatial) standard deviation (std) of the Northern Hemisphere Z500 difference between the control forecast and the verifying

analysis (i.e., the forecast error) for the period 29 April to 13 May 2001 is depicted in Fig. 7 (solid) along with the std of the total evolved Z500 key-analysis errors (dry and humidity key-analysis errors were applied). Evolved key-analysis errors are defined as the difference between the nonlinear sensitivity forecast and the control forecast. All results are based on the usage of the B norm. Obviously, the influence of humidity key-analysis errors only (based on diabatic sensitivity with moist B norm) on Northern Hemisphere Z500 is relatively small during the first few days of the forecast (Fig. 7, dash-dotted). In the far medium-range, however, evolved Z500 key-analysis errors due to humidity key-analysis errors amount to about 20–30% of the total forecast error. The magnitude of the total evolved key-analysis errors is much bigger than those for humidity key-analysis errors only; the magnitude is still smaller, though, than the forecast error throughout the whole forecast range. Summarizing, humidity key-analysis errors whose magnitude and structure is constrained by the B norm have only little impact on the nonlinear forecast compared to dry key-analysis errors.

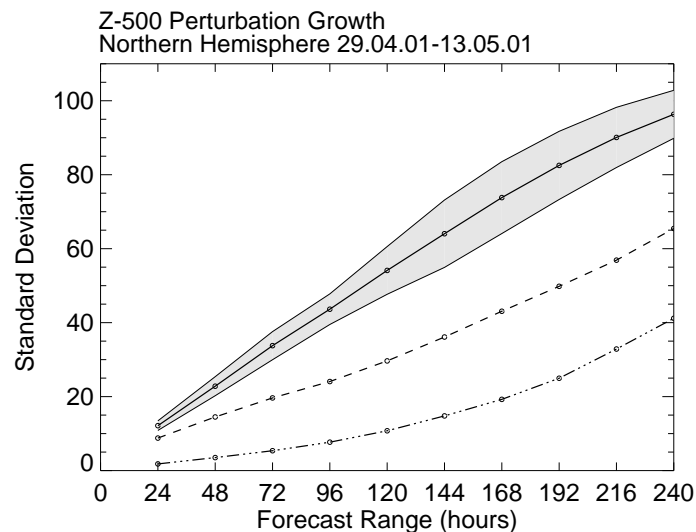


Figure 7: Mean standard deviation of Northern Hemisphere Z500 differences. Control forecast minus analysis (solid) with $\pm 1\sigma$ range (shaded). Evolved key-analysis errors (sensitivity forecast minus control forecast) using temperature, vorticity, divergence, surface pressure and humidity key-analysis errors (dashed). Evolved key-analysis errors using humidity key-analysis errors only (dash-dot). Statistics are based on the period from 29 April to 13 May 2001.

So far, the key-analysis errors were determined using an optimization time of 48 hours. It is worth asking whether the tangent linear hypothesis is valid for atmospheric humidity over this time range. To answer this question, three experiments were performed. The first experiment starts from the operational analysis (control forecast). In the second and third forecast experiment key-analysis errors have been added to and subtracted from the analysis, respectively. If the positive and negative perturbations evolve in the same manner except with opposite sign, then this can be seen as an indication for the linearity of the perturbations growth. The linearity, thus, can be measured by the spatial correlation coefficient (r). Fig. 8 shows r for every day from 29 April to 13 May 2001 for humidity perturbations at 700 hPa. For 48 hours forecasts, r lies in the range from -0.5 to -0.7 , that is, less than 50% of the variance of the negative perturbations can be explained by the positive perturbations. Evolved humidity key-analysis errors, therefore, are already noticeably distorted by nonlinearity after 2 days. This holds despite of the fact that the magnitude of the humidity key-analysis errors is relatively small (e.g., 0.2–0.4 g/kg at about 700 hPa, Fig. 4).

Experiments with shorter optimizations times (24 hours) have been performed (not shown). No reduction in the forecast errors compared to the control forecast has been found. This may be explained by the fact that the true forecast error after 24 hours is still relatively small so that analysis errors heavily affect the difference between the forecast and the analysis, this difference which is used as input in the adjoint calculation.

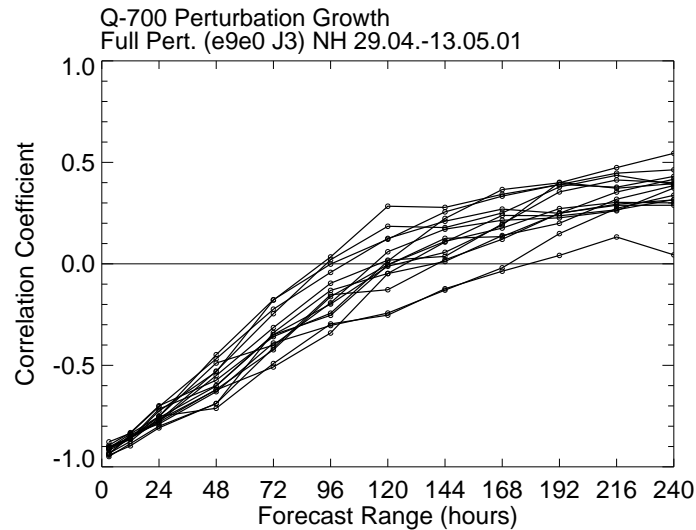


Figure 8: Correlation coefficient between positive and negative Northern Hemisphere evolved humidity key-analysis errors at 700 hPa for every day during the period from 29 April to 13 May 2001. Key-analysis errors for temperature, vorticity, divergence, surface pressure and humidity have been added to and subtracted from, respectively, the operational analysis. A correlation coefficient of -1 indicates linearity in the evolution of the key-analysis errors.

3.2 Moist extratropical singular vectors

Throughout the remainder of this section moist extratropical SVs are being discussed¹. The focus is on one particular severe weather event, namely the storm Lothar which, on 26 December 1999, led to serious damages in parts of France, Germany, and Switzerland. A description of the dynamics of ‘Lothar’ is given, for example, by Wernli et al. (2002).

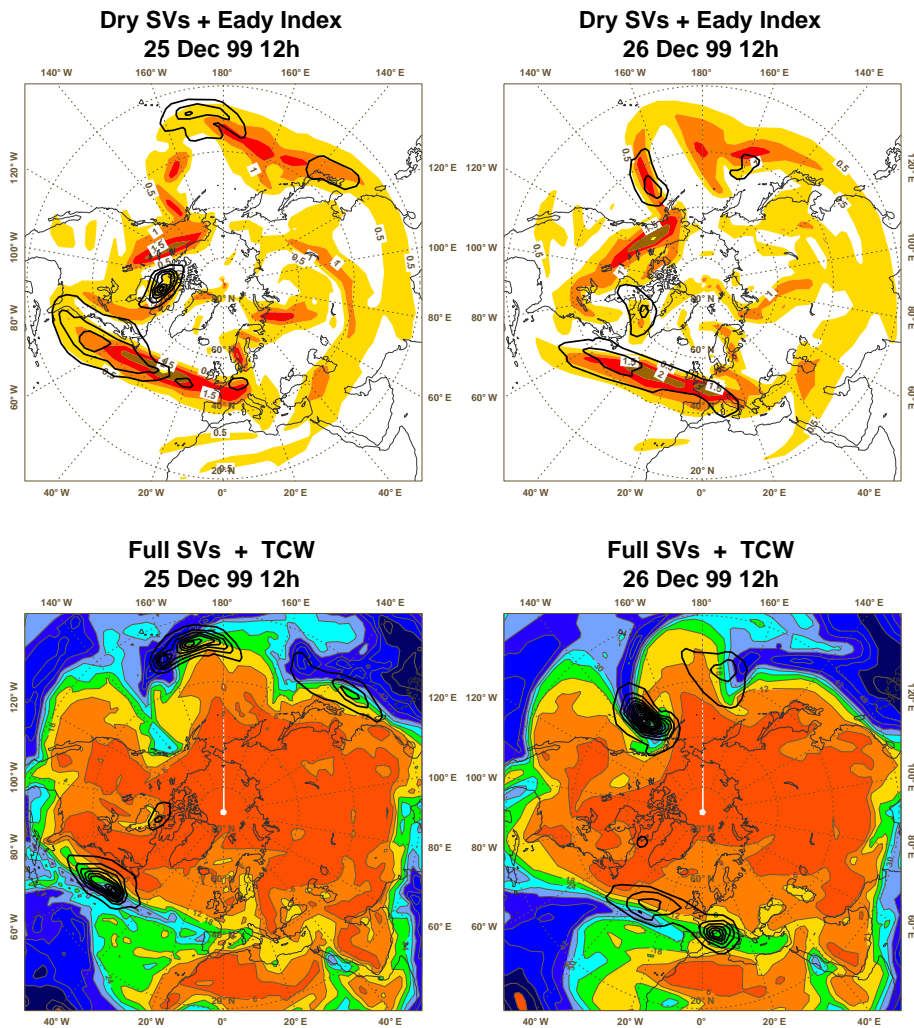
As for the sensitivity, first the impact of replacing the adiabatic (dry physics) TLP by a diabatic (full physics) counterpart is studied. Fig. 9 (upper row) gives the weighted (by the amplification factor) geographical distribution for the first 10 dry SVs superimposed on the baroclinicity index² at initial and final time. This shows that the SV structures are generally concentrated in regions of high baroclinicity. The computation with full physics, which is shown in Fig. 9 (lower row) superimposed on the basic state of total column water, lead to similar distributions. There are differences, though, between dry and moist SVs. The moist calculation shows a sensitive region near 50°W upstream of the tongue of moist air, which is more concentrated than those obtained by the dry calculation. One day later, perturbations from this region have moved under intensification into Middle Europe, giving a clearer indication for the occurrence of a severe weather event. The influence of moist processes is also seen for SVs in the North Pacific region; moist SVs, in some cases, are displaced towards the local moisture maximum.

Finally, the influence of including humidity perturbations (moist norm) in the diabatic SV computation has been studied. In Fig. 10 the geographical distribution of the leading 10 diabatic SVs at initial (left column) and final time (right column) is shown for the dry (no humidity perturbations, upper row) and moist norm (including humidity perturbations, lower row). The use of the moist norm results in larger SV growth; the spatial structure, though, is similar in both cases. Further investigation shows that the structures of individual SVs are very similar for computations with dry and moist norms. This suggests that the inclusion of initial humidity perturbations in the linearised calculations is of minor importance compared to a change from adiabatic towards diabatic singular vector computations. This conclusion has been confirmed for other severe weather cases in the European region.

¹The results on moist SVs are part of M.M. Coutinho’s PhD thesis.

²This index corresponds to the growth rate of the fastest growing normal mode in the Eady model (Hoskins and Valdes, 1990).

DISTRIBUTIONS OF ENERGY



Mariane Coutinho



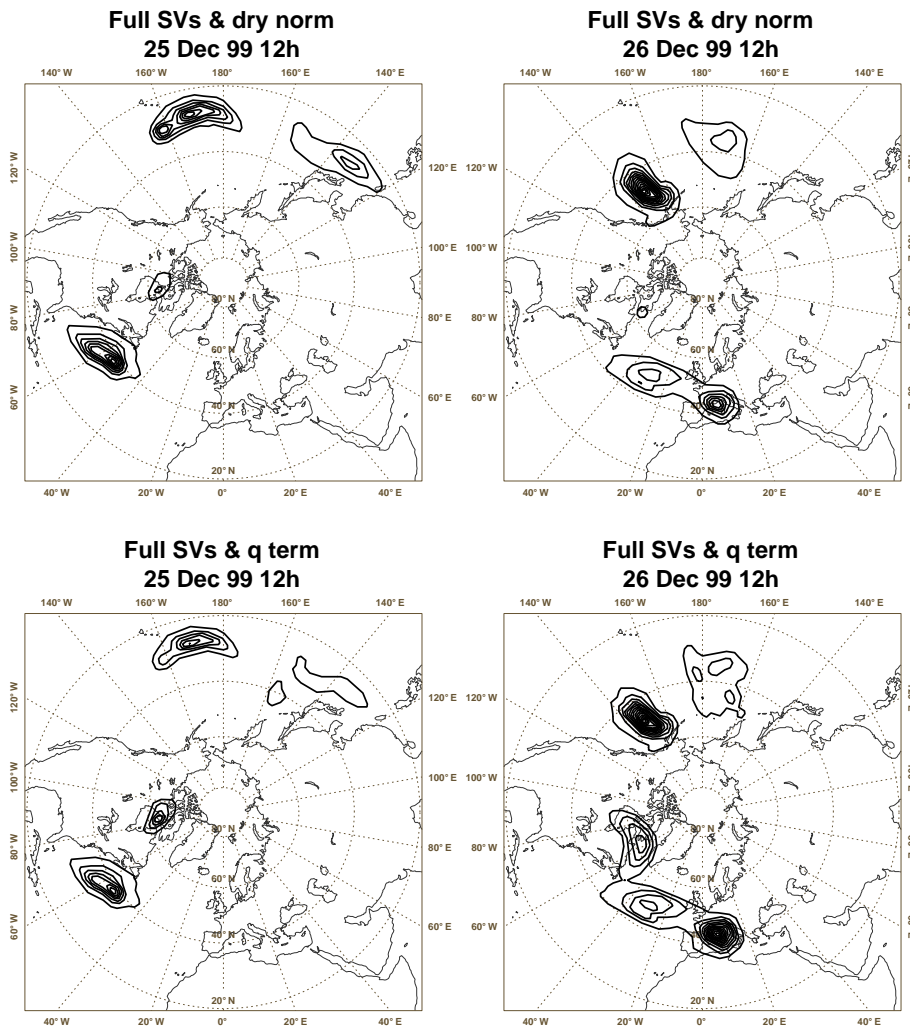
Figure 9: Geographical distribution of the amplification factor weighted total energy (contours) of the first 10 SVs at initial (left) and final (right) time for dry physics (top) and full physics (bottom). The contour interval at final time is 50 times that at initial time. A baroclinicity index (shaded, top) and the basic state for the total column water content (shaded, bottom) at initial time (left) and final time (right) are also shown.

4 Discussion

4.1 Sensitivity

The main conclusion of this study is that adiabatic and diabatic sensitivities give very similar results for dry and moist norms. It should be mentioned, however, that this conclusion has been drawn from statistics over 39 days for the Northern Hemisphere. It may well be the case that the inclusion of (linearized) diabatic processes is crucial for sensitivity computations, for example, when the sensitivity of targeted forecast errors (e.g., for developing cyclones) with respect to the initial conditions is being studied. It should be stressed that our results do not necessarily imply that diabatic processes are only of minor importance in terms of Northern Hemisphere forecast errors. First, the linearization of diabatic processes, which is necessary to formulate the TFP and its adjoint, is a non-trivial task. Second, if diabatic processes and humidity perturbations are taken into account,

DISTRIBUTIONS OF ENERGY



Mariane Coutinho



Figure 10: Geographical distribution of the amplification factor weighted total energy (contours) of the first 10 SVs at initial (left) and final (right) time using the dry (top) and moist (bottom) norm. The contour interval at final time is 50 times that at initial time.

then the linearity of the perturbation growth, and therefore the validity of the tangent linear hypothesis, may break down for relatively short optimization times (here 48 hours). These issues will be further addressed in a future study.

In this studies two different kinds of moist norms have been tested, that is, the moist TE norm and the B norm. The fact that the B norm leads to slightly improved nonlinear sensitivity forecasts suggests, that the B norm is more appropriate to describe key-analysis errors. For the future it is planned to use also the Hessian norm, which is similar to the B norm, but also takes into account observations to constrain key-analysis errors. For applications using moist norms there is another advantage of the B norm over the TE norm, that is, once the B norm has been formulated in the data assimilation context, there is no subjectivity associated with applications of the moist B norm, whereas for the moist TE the relative weight that is given to humidity perturbations has to be chosen more or less subjectively.

All sensitivity computations were based on the assumption that forecast errors are solely due to analysis errors

(perfect model assumption). First results using the so-called forcing sensitivity suggest, however, that model errors may have a non-negligible impact on forecast errors (Barkmeijer et al., 2003). To account for both, forecast errors due to analysis and model errors, it is planned to combine the regular sensitivity (Rabier et al., 1996) with the forcing sensitivity (Barkmeijer et al., 2003). This *joint* sensitivity should give better estimates of both, key-analysis and key-model errors.

4.2 Singular vectors

The inclusion of moist processes in linearised singular vector computations has a clear impact on the resulting SVs. Both, adiabatic and diabatic SVs tend to concentrate on region of high baroclinicity, but diabatic SVs are also influenced by the availability of moisture. The use of the moist norm has little impact on the resulting SV characteristics. The inclusion of humidity perturbations in the linear models results in larger growth rates, the spatial structures of the SV, however, are almost unchanged.

Acknowledgements

The authors would like to thank Erik Anderson, Roberto Buizza, Brian Hoskins, Ernst Klinker, and Tim Palmer for their useful comments.

References

- Barkmeijer, J., T. Iversen, and T. Palmer (2003). Forcing singular vectors and other sensitive model structures. *Quart. J. Roy. Meteor. Soc.*, submitted.
- Buizza, R. (1994). Localization of optimal perturbations using a projection operator. *Quart. J. Roy. Meteor. Soc.* 120, 1647–1682.
- Buizza, R. and T. Palmer (1995). The singular-vector structure of the atmospheric global circulation. *J. Atmos. Sci.* 52, 1434–1456.
- Buizza, R., T. N. Palmer, J. Barkmeijer, R. Gelaro, and J.-F. Mahfouf (1996). Singular vectors, norms and large-scale condensation. In *11th Conference on Numerical Weather Prediction, Norfolk, Virginia*, pp. 50–52. American Meteorological Society. AMS-Preprint Volume.
- Derber, J. and F. Bouttier (1999). A reformulation of the background error covariance in the ECMWF global assimilation system. *Tellus 51A*, 195–221.
- Ehrendorfer, M., R. Errico, and K. Raeder (1999). Singular-vector perturbation growth in a primitive equation model with moist physics. *J. Atmos. Sci.* 56, 1627–1648.
- Hoskins, B. J. and P. J. Valdes (1990). On the Existence of Storm-Tracks. *J. Atmos. Sci.* 47, 1854–1864.
- Klinker, E., F. Rabier, and R. Gelaro (1998). Estimation of key analysis errors using the adjoint technique. *Quart. J. Roy. Meteor. Soc.* 124, 1909–1933.
- Molteni, F., R. Buizza, T. Palmer, and Petroliagis (1996). The ECMWF ensemble prediction system: Methodology and validation. *Quart. J. Roy. Meteor. Soc.* 122, 73–119.
- Palmer, T. N. (2000). Predicting uncertainty in forecasts of weather and climate. *Rep. Prog. Phys.* 63, 71–116.
- Rabier, F., E. Klinker, P. Courtier, and A. Hollingsworth (1996). Sensitivity of forecast errors to initial conditions. *Quart. J. Roy. Meteor. Soc.* 122, 121–150.

Wernli, H. and H. C. Davis (1997). A Lagrangian-based analysis of extratropical cyclones. i: The method and some applications. *Quart. J. Roy. Meteor. Soc.* 123, 467–489.

Wernli, H., S. Dirren, M. A. Liniger, and M. Zillig (2002). Dynamical aspects of the life cycle of the winter storm ‘Lothar’ (24–26 december 1999). *Quart. J. Roy. Meteor. Soc.* 128, 405–429.